800-MeV inelastic proton scattering from ^{40}Ca, ^{48}Ca, and ^{54}Fe

G. S. Adams,* Th. S. Bauer,† G. Igo, G. Pauletta, C. A. Whitten, Jr., and A. Wriekat

Physics Department, University of California, Los Angeles, California 90024

G. W. Hoffmann

Physics Department, University of Texas, Austin, Texas 78712
and Los Alamos Scientific Laboratory, Los Alamos, New Mexico 87545

G. R. Smith

Physics Department, University of Colorado, Boulder, Colorado 80302

M. Gazzaly‡

Physics Department, University of Pennsylvania, Philadelphia, Pennsylvania 19174
(Received 15 November 1979)

Differential cross sections have been measured over a wide range of angles for the well resolved and/or strongly excited peaks in the inelastic proton spectra from ^{40}Ca, ^{48}Ca, and ^{54}Fe targets. Inelastic analyzing powers were also measured for the ^{54}Fe transitions. Microscopic distorted-wave impulse approximation analyses of the 2_1^+ transitions in ^{48}Ca and ^{54}Fe yield values for the ratio $B(N2)/B(E2)$. Collective-model distorted-wave Born-approximation calculations for the high-spin levels at 8.85 and 9.24 MeV in ^{40}Ca suggest spin and parity assignments of 6^+ and 5^-, respectively.

$$\left[\begin{array}{l} \text{NUCLEAR REACTIONS } ^{40,48}\text{Ca, } ^{54}\text{Fe}(\vec{p},p'); \text{ measured } \sigma(\theta), A(\theta); \text{ deduced opti-} \\ \qquad\qquad \text{cal-model parameters, } B(N2), \text{ DWBA analysis.} \end{array} \right]$$

I. INTRODUCTION

One of the primary reasons for extending proton-nucleus scattering measurements to intermediate energies is the hope that unambiguous information about nuclear wave functions can be deduced from the data. Theoretical descriptions of intermediate-energy proton-nucleus scattering are much simpler than their low-energy counterparts.[1] In particular, the effective nucleon-nucleon (N-N) interaction more closely resembles the free N-N interaction as the projectile energy is raised.[2]

Although proton-nucleus elastic scattering at intermediate energies has been extensively studied for the purpose of extracting ground-state neutron density distributions,[3,4] this technique has seldom been applied to the study of neutron transition densities via inelastic scattering. The fact that proton inelastic scattering is sensitive to the shape of the nuclear transition density will be demonstrated from the analysis of new 800-MeV (p,p') data. Angular distributions for a variety of transitions in ^{40}Ca, ^{48}Ca, and ^{54}Fe have been measured and theoretical analyses based on the distorted-wave Born approximation (DWBA) have been performed. While most of these data are well reproduced by calculations which assume a collective-model form factor, some transitions

require a more microscopic treatment of the transition density.

II. EXPERIMENTAL PROCEDURE

Data were obtained using the high resolution spectrometer at the Clinton P. Anderson Meson Physics Facility. The beam energy, 800 ± 2 MeV, was determined by measuring the kinematic energy difference resulting from elastic scattering from ^{40}Ca and ^{16}O targets. Differential cross sections and analyzing powers (^{54}Fe only) were measured out to a maximum momentum transfer q of 3.4 fm^{-1}. During the analyzing power measurements the transverse beam polarization P was continuously monitored by measuring the ^{1}H($\vec{p},p$) analyzing power, using a thin CH$_2$ target located upstream from the scattering chamber. The average value for P was 76%.

Measurements were performed at laboratory scattering angles from 4° to about 24°. These data were sorted into 0.5° scattering angle bins (three bins per spectrometer setting) by off-line analysis. The relative uncertainty in the scattering angle points is estimated at $\pm 0.015°$. The absolute scattering angle was determined by normalizing to published ^{12}C($\vec{p},p$) data,[5] resulting in an absolute uncertainty of $\pm 0.07°$. Excitation energies up to at least 15 MeV were
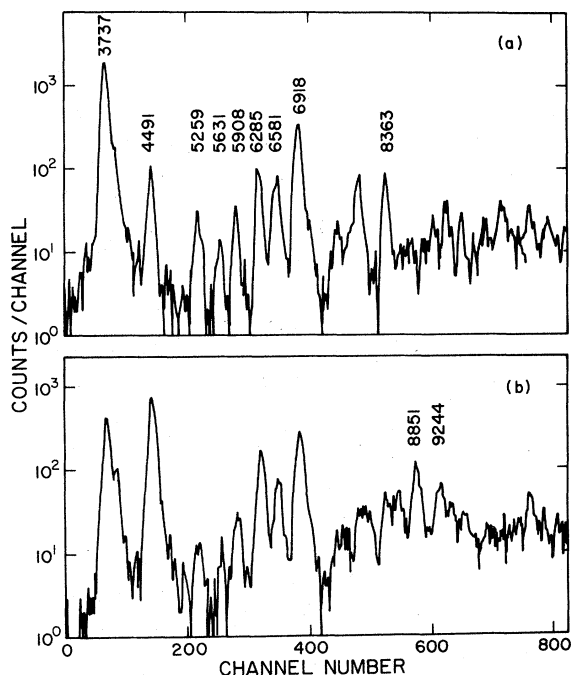
FIG. 1. Inelastic proton spectra from ^{40}Ca(p,p') at laboratory scattering angles of 8° (a) and 13.5° (b). The energy scale is approximately 10 keV per channel and the excitation energies of some of the strong peaks are given in keV.

measured in all three targets. Sample spectra are shown in Figs. 1 and 2. Typical energy resolutions for these measurements were 105, 130, and 140 keV full width at half maximum (FWHM) for ^{40}Ca, ^{48}Ca, and ^{54}Fe, respectively. Fixed lineshape peak fitting programs were used to extract peak areas for excitation energies up to 12.5, 9.0, and 6.5 MeV in these respective nuclei. Angular distributions will be presented for those peaks that are dominated by a single state, plus the 5.26 and 6.92 MeV doublets in ^{40}Ca. Cross sections
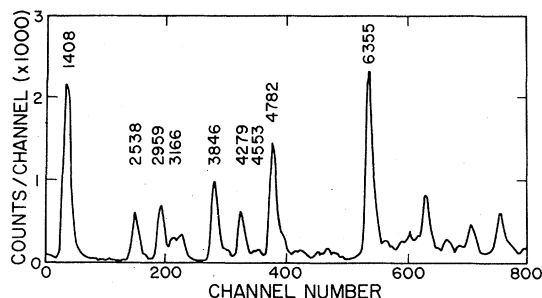

FIG. 2. Inelastic proton spectrum from ^{54}Fe$(\vec{p},p')$ at 8° (laboratory). This spectrum is composed of the sum of both beam polarizations, with scattering angle bin $\simeq 1.5°$. The energy scale is approximately 10 keV per channel and the excitation energies of some of the strong peaks are given in keV.

for these transitions were measured relative to the count rates in two plastic-scintillator monitor telescopes which viewed the target at scattering angles of plus and minus 80°. These cross sections were normalized absolutely to the elastic cross sections of Refs. 6 and 7 at laboratory scattering angles $\gtrsim 8°$, with relative uncertainties of about $\pm 4\%$ in each case. Adding these errors in quadrature with the ten percent uncertainties present in the published elastic scattering data[6,7] yields absolute cross section uncertainties of $\pm 12\%$ for ^{40}Ca and $\pm 11\%$ for ^{48}Ca and ^{54}Fe.

Excitation energies for high-lying levels were determined relative to several well known levels in the same nucleus.[8-10] These calibration levels are indicated by parentheses in Table I.

Targets of isotopically enriched ^{40}Ca ($>99.9\%$), ^{48}Ca (94.5%), and ^{54}Fe (97.6%) were used for the present measurements. Target thicknesses were 48, 101, and 97 mg/cm^2, respectively. A 5.3% ^{40}Ca contamination in the ^{48}Ca target was the only noteworthy contaminant in any of the targets. Substantial contributions from the 3_1^- excitation in ^{40}Ca were subtracted from the ^{48}Ca 2_1^+ data.

III. DATA AND COLLECTIVE MODEL DWBA ANALYSIS

Figures 3–8 show the differential cross sections and analyzing powers measured in this experiment. One interesting feature of these data is the variety of shapes exhibited in the angular distributions for transitions having the same orbital angular momentum transfer, L. The best examples are the 3^- transitions in ^{40}Ca and the 2^+ transitions in ^{54}Fe. This variety is not exhibited in the ^{40}Ca (α, α') data of Rutledge and Hiebert,[14] probably because the alpha particle is more strongly absorbed than an 800-MeV proton.

The solid curves in Figs. 3 through 8 are the results of collective-model DWBA calculations in which the form factors are proportional to the derivative of the elastic scattering optical potentials. The parameters of these phenomenological optical potentials, given in Table II, were fitted to the elastic differential cross section and polarization data of Refs. 6 and 7. The elastic and inelastic analyses used relativistic kinematics,[15] and the deformed spin-orbit amplitude was included in the DWBA using the full Thomas form.[16] Spin-orbit and central deformation parameters were set equal to one another. The importance of the spin-orbit amplitude for 800-MeV protons has been previously emphasized.[17,18] Program constraints limited the number of partial waves used in the DWBA calculations to 50. Because of this limitation, only the results for scattering angles less than 20° were deemed accurate. This limit was determined by calculations with a different pro-

TABLE I. Deformation lengths δ_L $(=\beta_L R_{optical})$ from collective-model DWBA analyses.

Nucleus	J^π	E_x^a (keV)	E_x^b (keV)	δ_L^b (fm)	δ_L^c (fm)
^{40}Ca	0^+	3352	(3352)		
	3^-	3737	(3737)	1.39	1.32
	2^+	3904	3915 ± 12	0.52	0.43
	5^-	4491	(4491)	0.76	0.80
	0^+	5213			
	2^+	5249	5259 ± 10		0.12
	4^+	5279			0.13
	4^-	5614			
	2^+	5630	5631 ± 5	0.15	
	1^-	5903	5908 ± 13		
	2^-	6026			
	3^+	6029			
	3^-	6285	(6285)	0.38	0.40
	4^+	6508			0.17
	4^+	6543			
	3^-	6583	6581 ± 10	0.34	0.32
	2^-	6751	6700 ± 42		
	2^+	6909		0.49	0.45
		6927			
	(6^+)	6930	6918 ± 20		
		6938			
	1^-	6951			
	4^+	8373	8363 ± 13	0.35	0.33
	$(6-8)^+$	8851	8851 ± 9	$\delta_6 = 0.28$	$\delta_7 = 0.09$
	$(6-8)^-$	9237	9244 ± 9	$\delta_5 = 0.23$	$\delta_7 = 0.06$
^{48}Ca	2^+	3832	(3832)	0.64	0.70
	0^+	4284			
	(4^+)	4503			
	3^-	4507	4518 ± 20	0.87	0.81
	3^-	5370	5376 ± 25	0.41	0.46
	0^+	5461			
	5^-	5729	(5729)	0.38	0.46
^{54}Fe	2^+	1408	(1408)	0.86	0.75
	4^+	2538	(2538)	0.36	
	0^+	2561			
	6^+	2950			
	2^+	2959	(2959)	0.51 [d]	0.67
	2^+	3166	(3166)	0.30	
	4^+	3295			
	3	3345			
	4^+	3834	3846 ± 15	0.43	
	(4^+)	4033			
	4^+	4047			
	3	4072			
	4^+	4263	4279 ± 18	0.35	
	(0)	4292			
	2^+	4578	4553 ± 36	0.26	
	(2^+)	4655			
	3^-	4780	4782 ± 12	0.47	0.54
	3^-	6335	6355 ± 14	0.63	0.67

[a] Excitation energies and J^π values from Refs. 8, 9, and 10.
[b] Present work. For the 800-MeV analysis $\delta_L \equiv \beta_L r_i A^{1/3}$.
[c] See Refs. 11, 12, and 13.
[d] Add these numbers in quadruture for comparison with the value on the right.
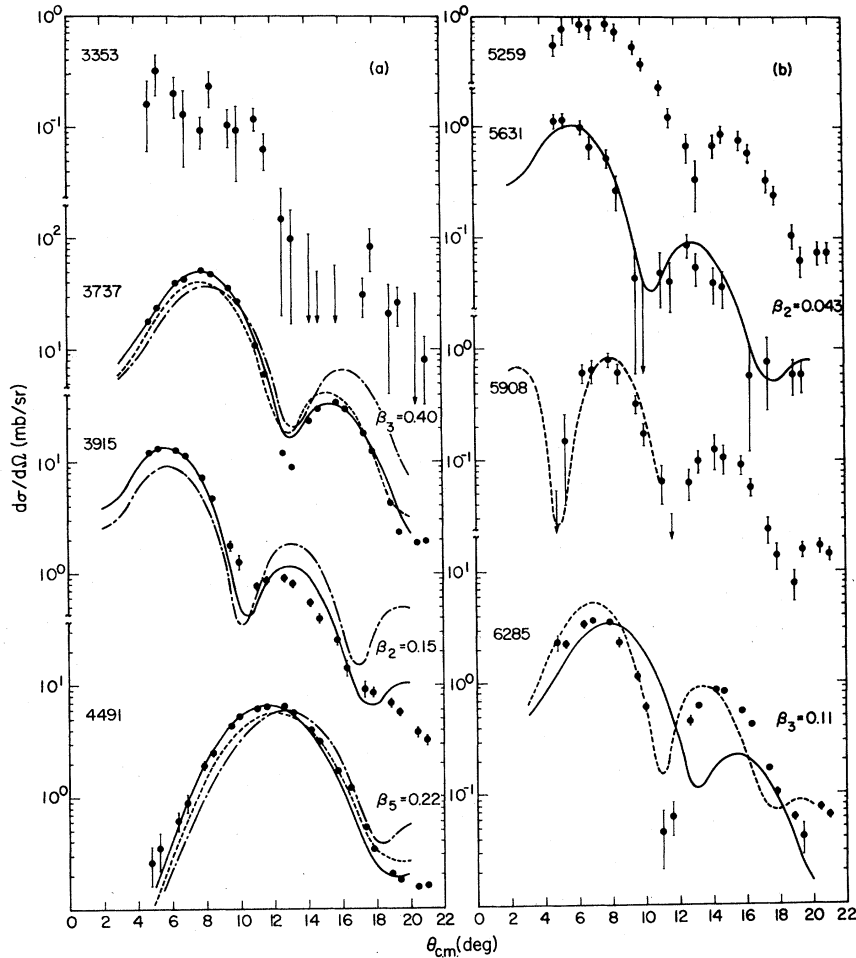
FIG. 3. Angular distributions for excitations in ^{40}Ca. Solid lines are the results of collective-model DWBA calculations with β_L indicated for each case. The remaining curves (described in the text) are the results of microscopic DWIA calculations.

gram which allowed more partial waves to be included but did not have provisions for a spin-orbit transition operator.

The DWBA results, including deformation parameters (β_L^2 = measured rate/calculated rate), are given in Figs. 3 through 8. Very good agreement was obtained between the shapes of the DWBA predictions and the measured angular distributions for most transitions. Table I summarizes the present results and compares them with the low-energy proton results of Refs. 11–13. The deformation length $\delta_L (=\beta_L R_{optical})$ was chosen as the most unambiguous parameter for comparison. For the present analysis $R_{optical} = r_i A^{1/3}$. This comparison reveals that the results of the 800-MeV analysis are in good agreement with most of the low-energy work. It should be mentioned that considerable variation exists in the published deformation lengths for the ^{54}Fe transitions.[10] Our results show better agreement with the results of Fricke

and co-workers[13] than with those of some other authors (see the compilation in Ref. 10).

More interesting than this general confirmation of the distorted-wave method are those exceptional cases in which the DWBA fails to reproduce the data. The best examples are the $J^\pi_N = 2^+_1$, 4^+_1, 3^-_2, and 3^-_3 transitions in ^{40}Ca, with excitation energies of 3.91, 5.26, 6.28, and 6.58 MeV, respectively. The failure in the case of the 2^+_1 state manifests itself in predicted cross sections that are too oscillatory at large angles. Note also that the present deformation length is considerably larger than the value deduced by Gruhn *et al.*[11] Based on low-energy proton scattering results,[11] the peak at 5.26 MeV is expected to have substantial contributions from both the 2^+_2 and the 4^+_1 states. It was not possible to achieve a reasonable fit to the present data using a sum of $L = 2$ and $L = 4$ distributions. The presence of a minimum in the measured angular distribution at $13.5°$ is particu-
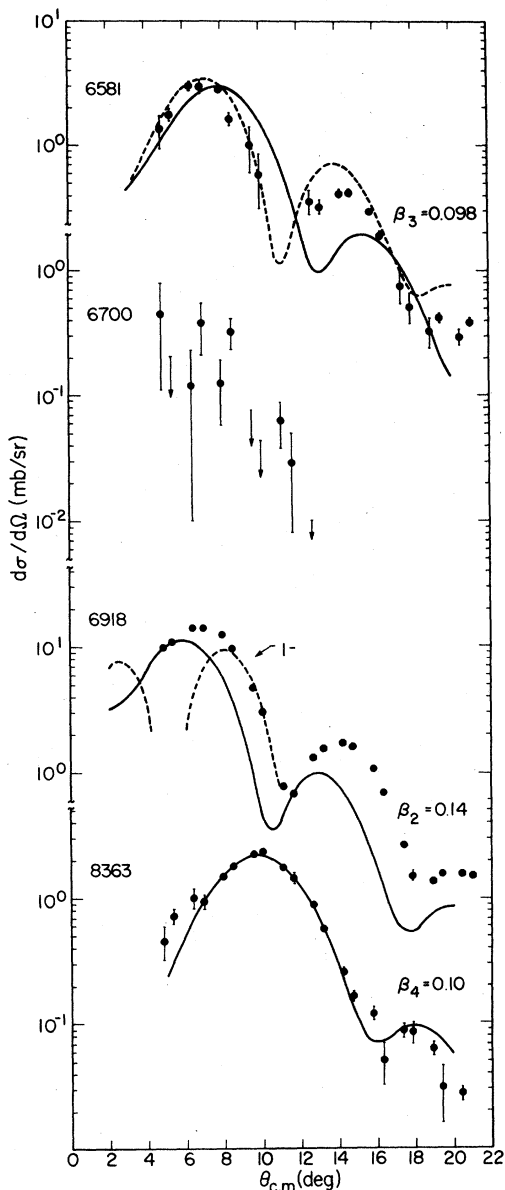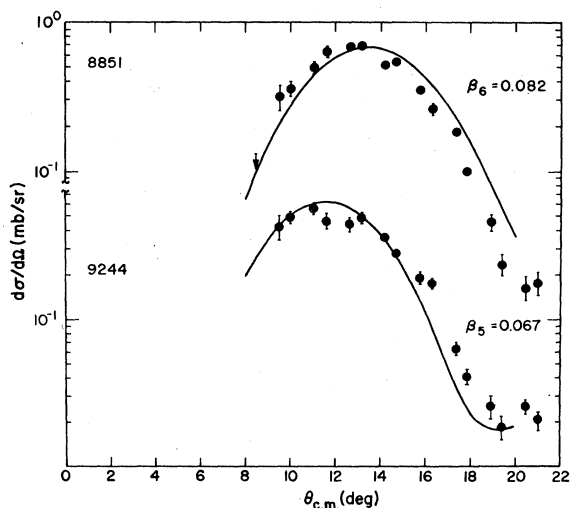
FIG. 4. Same as Fig. 3.

FIG. 5. Angular distributions for the high-spin states in ⁴⁰Ca. The theoretical curves are the best-fit DWBA results, with β_L indicated for each case.

larly restrictive. Since a sum of $L = 2$ and $L = 3$ distributions with $\beta_2 = 0.027$ and $\beta_3 = 0.048$ provided a much better description of the data, we conclude that an anomalous 4^+ angular distribution is the source of difficulty. As the 2^+_1 and 4^+_1 states in ⁴⁰Ca are members of a $K^\pi = 0^+$ rotational band,[19] it appears likely that the neglect of coupled-channels effects may be the cause of the disagreement between the DWBA and the data for these two transitions. Previous analyses of inelastic proton scattering from ¹²C (Ref. 20) and ⁵⁸Ni (Ref. 21) have demonstrated the importance of such effects for 800-MeV protons. The analysis presented in

the next section shows that the discrepancies observed between the DWBA calculations and the 3^-_2 and 3^-_3 data are due to the fact that these states have wave functions that are quite different from those produced by the collective model.

Other interesting features of the present data are the weak excitation of the 2^- state at 6.7 MeV in ⁴⁰Ca, and the strong excitation of the levels at 8.85 and 9.24 MeV (see Figs. 4 and 5). Although the 2^- peak was not resolved from the adjacent peaks at 6.58 and 6.92 MeV in any of the measured spectra, its presence was required at several angles in order to obtain good peak fitting results. In view of this fact, we assign an absolute cross section uncertainty of $\pm 50\%$ to the 2^- data. The levels at 8.85 and 9.24 MeV are known to have high spin; low-energy (p, p') work suggests $L = 7$ for both of these levels.[11] Spin and parity assignments of 6^- have also been suggested by the low-energy work because the $(d_{5/2}^{-1}, f_{7/2})$ "stretched" configuration produces the states with highest spin in a 1-$\hbar\omega$ particle-hole basis. Since the corresponding 6^- states[22] are not strongly excited by 800-MeV proton scattering from ²⁴Mg and ²⁸Si,[23] this assignment is unlikely for these strong ⁴⁰Ca excitations. We also observe no measurable excitation of the stretched 8^- state located at 13.26 MeV in ⁵⁴Fe.[24] Figure 5 shows the DWBA results for the ⁴⁰Ca transitions. The best agreement between the DWBA and the data was obtained with $L = 6$ and $L = 5$ for the 8.85 and 9.24 MeV transitions, respectively. However, an $L = 6$ assignment for the 9.24-MeV state cannot be ruled out. In view of these results we suggest that the states at 8.85 and 9.24 MeV have natural parity, with probable J^π assignments of 6^+ and 5^-, respec-
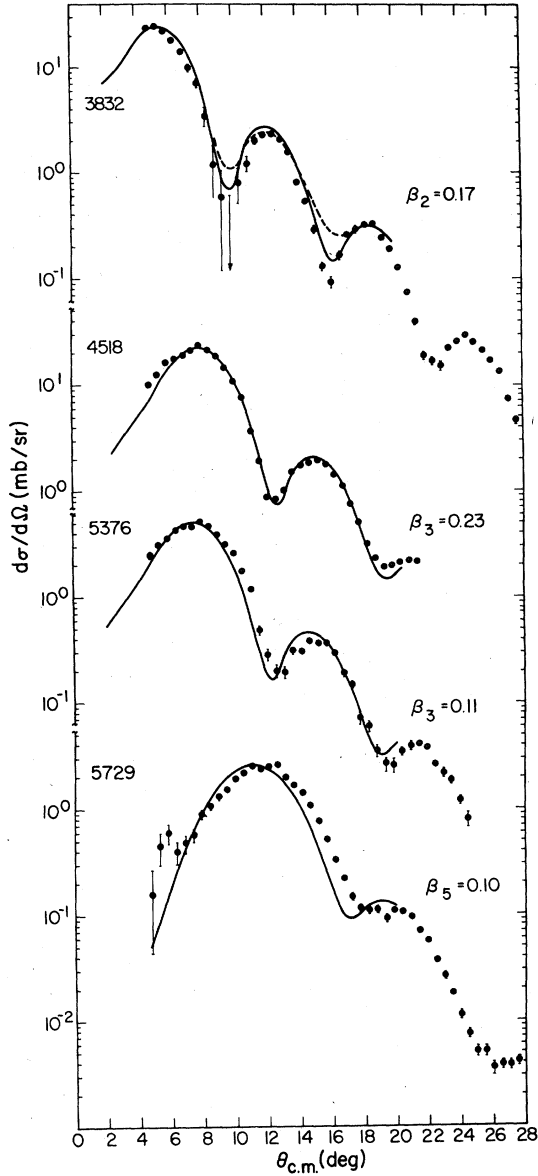
FIG. 6. Same as Fig. 3, but for ^{48}Ca.

tively. Large-angle (e,e') and (α,α') measurements coupled with the present data would provide unambiguous spin, parity, and isospin assignments for these states. Forthcoming asymmetry data should also prove interesting since, as one can see from Fig. 8, the DWBA is able to reproduce the analyzing powers for a variety of natural-parity transitions rather well.[17]

IV. DWIA ANALYSIS

Distorted-wave impulse approximation (DWIA) calculations for some natural-parity transitions were carried out following the approach of Hay-

bron, Johnson, and Metzger.[25] Empirical proton transition densities ρ_p resulting from fits to inelastic electron scattering data were used in these calculations. The parameters of the neutron density ρ_n were either set equal to the proton ones (as for ^{40}Ca) or adjusted to fit the (p,p') data. Although this method has been applied to a number of lower-energy (p,p') studies,[26] it has received only limited application in the region of 1-GeV proton energy.[4] Similar studies of intermediate-energy proton[27] and alpha[28] inelastic scattering have been carried out in the Glauber formalism. Exchange effects were included implicitly through the use of a symmetrized N-N t matrix,[1,3,4] a procedure which is known to be valid at high energies.[1,3,4,29] Contributions from the spin-spin parts of the nucleon-nucleon t matrix were neglected,[4] as were the small S-1 spin-orbit amplitudes.[18,30] The distorted waves were again generated with the optical potentials of Table II.

A. ^{40}Ca

Analyses[3,4] of proton elastic scattering data[6,31] are consistent with the assumption that the ground-state neutron and proton distributions of ^{40}Ca are approximately equal. Therefore, in the present investigation the approximation $\rho_n = \rho_p$ was deemed sufficiently accurate for the low-lying excited states of ^{40}Ca as well. Thus the ^{40}Ca data will provide a test of the DWIA approach which is relatively insensitive to nuclear structure uncertainties. The N-N t matrix was taken from the elastic scattering analysis of Ray,[3] the spin-orbit part having been fitted to the 800-MeV p + ^{40}Ca elastic scattering data, with appropriate adjustments for the p+ nucleus center-of-mass frame.[4] The empirical charge transition densities ρ_{ch} were also taken from the literature. Figure 3 shows the effect of assuming different shapes for ρ_{ch}. The dot-dash and dashed curves for the 3_1^- and 2_1^+ transitions used Tassie[32] and shell-model[33] shapes, respectively. The dot-dash and dashed curves for the 5_1^- transition show a similar comparison using Gaussian[34] and shell-model ($\alpha = 0$ fit in Ref. 33) shapes, respectively. Striking differences are observed, particularly at high momentum transfers, between the different calculations and between some of the calculations and the (p,p') data. The differences between the calculations are due to the differences in the shapes of the transition densities. These shape differences arise primarily from a dependence of the electron scattering analyses on the range of momentum transfer q spanned by the data. Generally only the first maximum in the momentum-space form factors is well determined. One
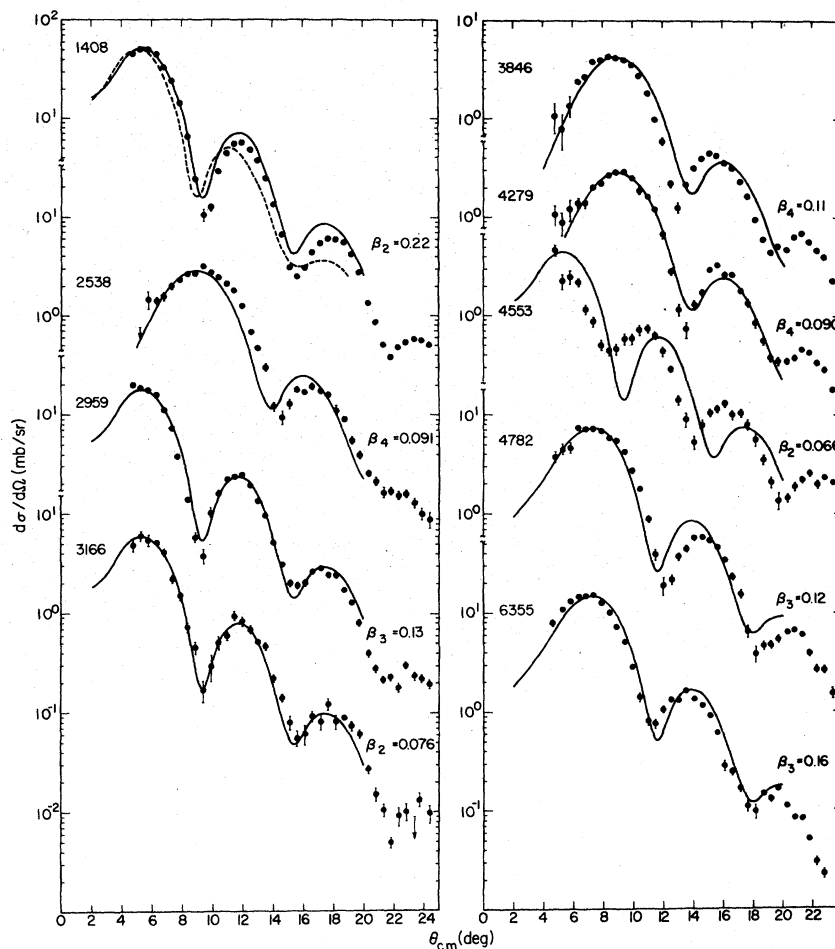
FIG. 7. Same as Fig. 3, but for ⁵⁴Fe.

might expect that the (p,p') distributions would not be very sensitive to the high-q parts of the transition densities because the incident and out-going proton waves are strongly distorted by the nuclear optical potential. Obviously this is not the case for the low-lying states in ⁴⁰Ca. Other examples are the 3_2^- and 3_3^- states. The predictions for these transitions, shown as dashed curves in Figs. 3 and 4, also used the shell-model transition densities of Itoh, Oyamada, and Tori-zuka.[33] In these cases the (p,p') data clearly demonstrate the same distinctive large-q enhancement that is present in the electron scattering form factors.[33] Such features do not appear in the (α,α') angular distributions[14] for these excitations, however, they can be observed in 135-MeV (p,p') data[35] and may be discernable in the low-energy proton data of Ref. 11.

The remaining DWIA calculations were for the 1⁻ states at 5.91 and 6.92 MeV. For these cases ρ_{ch} had the form

$$\rho_{ch} = C\left(\frac{1}{r^2}\frac{d}{dr}(r^3\rho)\right),$$ (1)

where C was determined by normalizing to the maximum in the (e,e') form factors,[33] and ρ was the ground-state density of Frosch et al.[36] Since this shape is not well determined at large q, the proton calculations were not extended beyond 11°. From Figs. 3 and 4 we observe that these calculations are in good agreement with the data, provided the excitation of both the 2⁺ (6.91 MeV) and the 1⁻ (6.95 MeV) states are accounted for in the 6.92 MeV peak. Unlike the ¹⁶O 1_1^- excitation,[18] the predicted minimum in the angular distribution for the 5.91 MeV state is present in the data. The overall agreement between the proton data and those DWIA calculations depicted by dashed curves in Figs. 3 and 4 is very encouraging. We interpret these results as a confirmation of the validity of the DWIA method in its present (approximate) form.
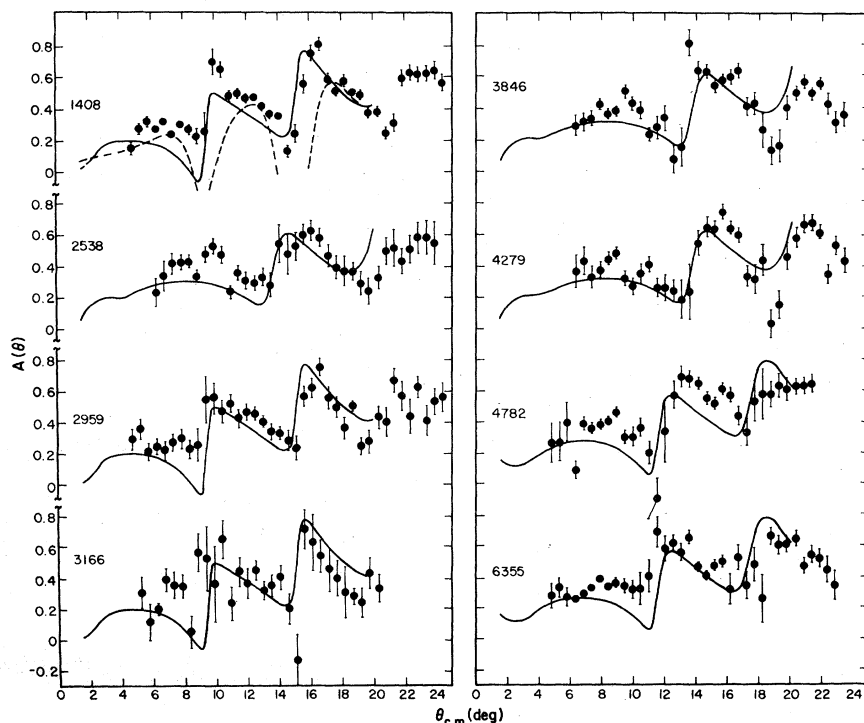
G. S. A D A M S *et al.*

FIG. 8. Analyzing powers for excitations in ^{54}Fe. Solid lines are the results of collective-model DWBA calculations with $\beta_{so} = \beta_{central}$. The dashed curve is the result of a microscopic DWIA fit to the differential cross sections for the 2_1^+ transition.

B. ^{48}Ca

Having verified that the ^{40}Ca data are amenable to a DWIA approach, it is then possible to use the same method to study those cases for which $\rho_n \neq \rho_p$. Such a study has been carried out on a variety of nuclei by Chaumeaux, Layly, and Schaeffer[4] using 1-GeV proton scattering data.[4,31] Few electron scattering data exist for ^{48}Ca, however, Eisenstein *et al.*[37] have measured the small-q form factors of the low-lying states and fitted them with a Tassie-model shape. The resulting ρ_{ch} for the 2_1^+ state was used in the DWIA calculation of the (p,p') distribution.

Two choices for the N-N spin-orbit interaction were tried in the DWIA calculations, resulting in only minor differences in the predicted cross sec-

tions. Since the structure calculations of Ref. 38a and the results of the present analysis suggest that the isospin composition of the 2_1^+ state in ^{48}Ca could be very different from that of the ground state, the N-N parameters of "solution 1" in Ref. 3 were chosen over the isospin-averaged interaction of Ref. 6 for the analysis presented below. These parameters were fitted to the free N-N scattering data.

The Tassie-model parameters of ρ_n were adjusted to reproduce the proton data, with the final results depicted in Fig. 6. Although the overall fit to the data is reasonably good, one can observe interesting discrepancies in the regions of the minima. An important quantity which can be deduced from this fit is the neutron equivalent of the $B(E2)$ value $B(N2)$, where

TABLE II. Phenomenological optical-model parameters. The convention followed is that of Perey and Perey [At. Data Nucl. Data Tables 13, 293 (1974)]. No investigation of possible fitting ambiguities was made.

Nucleus	V (MeV)	W (MeV)	V_{so} (MeV)	W_{so} (MeV)	r_0 (fm)	a_0 (fm)	r_i (fm)	a_i (fm)	r_{so} (fm)	a_{so} (fm)	r_c (fm)
^{40}Ca	−4.40	66.6	0.64	2.34	0.89	0.69	1.01	0.61	0.98	0.65	1.05
^{48}Ca	−2.02	64.0	0.74	1.71	1.05	0.55	1.03	0.59	1.03	0.57	1.05
^{54}Fe	−3.39	65.9	0.73	1.72	0.94	0.69	1.04	0.57	1.01	0.65	1.05

$$B(NJ) \equiv (2J+1) \left| \int_0^\infty \rho_n r^{J+2} dr \right|^2 . \qquad (2)$$

This quantity is proportional to ρ_n^2 at q equal to zero. In the fit to the proton data it was most sensitive to the overall magnitude of $\rho_n(q)$ and hence to the peak cross section in the proton angular distribution. The resulting value of $B(N2) = 877\ e^2\,\mathrm{fm}^4$ is likely very model dependent. Since the final shapes for ρ_n and ρ_p are similar, a less model dependent quantity is $B(N2)/B(E2) = 10.2 \pm 3.0$.[38b] The error in this ratio is composed of a 12% uncertainty in $B(E2)$,[37] an 18% error in $B(N2)$ for proton cross section normalization uncertainty, and a 20% error in $B(N2)$ due to ambiguities in the fitted parameters of ρ_n. One further source of error that is difficult to determine is the uncertainty in the q dependence of ρ_{ch}. The electron scattering data[37] do not span the necessary range of momentum transfer to determine ρ_{ch} in the region covered by the proton data, and this results in a correlated uncertainty in the deduced value of $B(N2)$. Because of these uncertainties it is useful to compare $\rho_n(q)$ with $\rho_p(q)$ near their maxima. Such a comparison does not require large extrapolations of either the electron or proton fits. Also, multiple scattering effects are minimal near the maximum in ρ_n.[4] In fact, at $q = 0.8\ \mathrm{fm}^{-1}$ the ratio $\rho_n^2/\rho_p^2 = 6.7$ may be a better estimate of the ratio $B(N2)/B(E2)$ than the value deduced above. Contributions to the error in $B(N2)/B(E2)$ due to uncertainties in the N-N amplitudes and second order transitions have been omitted,[4] as have contributions due to model dependence.

Both of the above mentioned estimates of $B(N2)/B(E2)$ are surprisingly large results. They are considerably larger than the values deduced by the same technique for the 2_1^+ states in ^{40}Ca, ^{44}Ca, and a variety of Ni isotopes.[4] Unfortunately the present estimates are inconsistent with the DWBA analysis presented in Sec. III. Approximately equal β_2 values were deduced for the 2_1^+ transitions in both ^{40}Ca and ^{48}Ca, and the electron scattering analyses[37] yield approximately equal $B(E2)$ values as well. This implies that $B(N2)/B(E2) \simeq 1$ for the ^{48}Ca state. This inconsistency can be removed only if the DWBA method of analysis is shown to be inappropriate for the ^{40}Ca 2_1^+ transition (e.g., if coupled channels are important) or if large sources of error remain unaccounted for in the ^{48}Ca DWIA analysis. These 2_1^+ transitions warrant further theoretical study, as well as experimental investigation with electron and proton probes.

C. ^{54}Fe

Although a significant amount of ^{54}Fe (e,e') data has been published,[39] analysis of the proton data

is complicated by the absence of phenomenological fits to the electron scattering data. An approximate fit to the 2_1^+ charge form factor was obtained as follows. A Tassie-model shape with the parametrization

$$\rho_{ch} = Kr\frac{d}{dr}\left(1 + e^{(r-C)/Z}\right)^{-1}$$

was assumed. The value for Z was extrapolated from the ^{56}Fe value of Ref. 34 using the results of their Ca and Ti isotopic analyses, and C and K were fitted to the small-q data of Ref. 39 in a plane-wave calculation. Thus the resulting values of $Z = 0.692$ fm, $C = 3.48$ fm, and $B(E2) = 1159\ e^2\,\mathrm{fm}^4$ are not as well determined as one would like. In particular, one should note that this $B(E2)$ value is about 60% larger than what would have been obtained by normalizing the shell-model form factor of Ref. 39 to agree with their data, and is more than twice as large as the value determined by Morrison, Smith, and Amos.[40]

Two choices for the N-N spin-orbit interaction[3,7] were again tried in the DWIA calculations, resulting in only small differences in the predicted cross sections and hence in the deduced value of $B(N2)$. The isospin-averaged interaction of Ref. 7 produced inelastic analyzing powers that were in better agreement with the 2_1^+ data of Fig. 8 than those calculated with the solution 1 interaction of Ref. 3; therefore, the former was chosen for the analysis presented below. The parameters of this interaction were fitted to the 800-MeV ^{54}Fe(p,p) cross section and asymmetry data.[7]

In view of the large uncertainties present in the parameters of ρ_{ch} for the 2_1^+ excitation, fitting the proton cross section data by varying all of the parameters of ρ_n is not very instructive. Figures 7 and 8 show the results that were obtained by adjusting only the magnitude of ρ_n, assuming the same shape for ρ_n and ρ_p. As in the previous case the resulting value for $B(N2)$, $985\ e^2$ fm^4, shows little sensitivity to small changes in C and Z provided the maximum value of the (p,p') cross section is always reproduced. Using the $B(E2)$ value given above we obtain the ratio $B(N2)/B(E2) = 0.85 \pm 0.27$. The error is composed of a 10% uncertainty in $B(N2)$ due to an uncertainty in the peak magnitude of the electron scattering form factor, 15% uncertainties in each of $B(N2)$ and $B(E2)$ due to proton and electron fitting ambiguities, respectively, and a 21% error in $B(N2)$ due to proton absolute cross section uncertainty. No model dependence was included in the error analysis.

From Fig. 8 one can easily observe that the above procedure produces only qualitative agreement between the DWIA prediction and the 2_1^+ analyzing power data. This suggests that a pheno-

menological approach which fits the parameters of the spin-orbit t matrix to the inelastic analyzing power, rather than the elastic analyzing power, might be more appropriate.

V. SUMMARY AND CONCLUSIONS

Angular distributions for 800-MeV proton excitation of many discrete states in ^{40}Ca, ^{48}Ca, and ^{54}Fe have been presented. These data show a variety that is not present in low-energy alpha particle distributions. While the collective-model DWBA provides a good description of most of the data, its failures are not limited to those cases in which coupled channels effects are expected to be important. DWIA calculations using empirical electron scattering transition densities resolve some of these discrepancies and show an unexpected sensitivity to the shapes of the transition densities at large q. Full exploitation of

the DWIA method of analysis is hampered by the scarcity of high-resolution electron scattering data for targets of ^{48}Ca and ^{54}Fe. However, it was possible to extract values for the ratio of $B(N2)$ to $B(E2)$ for the 2_1^+ states by adjusting the parameters of ρ_n to fit the present data.

The relatively large strengths measured for the 8.85 and 9.24 MeV transitions in ^{40}Ca suggest that these are natural-parity states. Collective-model DWBA analyses of these states are consistent with $J^\pi = 6^+$ and 5^-, respectively.

*Present address: Department of Physics and Laboratory for Nuclear Science, Massachusetts Institute of Technology, Cambridge, Mass. 02139.

†Present address: CEN de Saclay, Gif-sur-Yvette, France.

‡Present address: Department of Physics, University of Minnesota, Minneapolis, Minn. 55455.

[1]A. K. Kerman, H. McManus, and R. M. Thaler, Ann. Phys. (N.Y.) 8, 551 (1959); G. R. Satchler, Nucl. Phys. 77, 481 (1966); R. J. Glauber, *High Energy Physics and Nuclear Structure*, edited by S. Devons (Plenum, New York, 1970), p. 207.

[2]G. Bertsch, J. Borysowicz, H. McManus, and W. G. Love, Nucl. Phys. A284, 399 (1977); W. G. Love *et al.*, Phys. Lett. 73B, 277 (1978); A. Picklesimer and G. Walker, Phys. Rev. C 17, 237 (1978).

[3]L. Ray, Phys. Rev. C 19, 1855 (1979), and references therein.

[4]A. Chaumeaux, V. Layly, and R. Schaeffer, Ann. Phys. (N.Y.) 116, 247 (1978), and references therein.

[5]G. S. Blanpied *et al.*, Phys. Rev. Lett. 39, 1447 (1977).

[6]G. Igo *et al.*, Phys. Lett. 81B, 151 (1979).

[7]G. W. Hoffmann *et al.*, Phys. Lett. 79B, 376 (1978).

[8]P. M. Endt and C. Van der Leun, Nucl. Phys. A310, 1 (1978).

[9]J. R. Beene, Nucl. Data Sheets 23, 1 (1978).

[10]H. Verheul and R. L. Auble, Nucl. Data Sheets 23, 455 (1978).

[11]C. R. Gruhn *et al.*, Phys. Rev. C 6, 915 (1972).

[12]C. R. Gruhn, T. Y. T. Kuo, C. J. Maggiore, and B. M. Preedom, Phys. Rev. C 6, 944 (1972).

[13]M. P. Fricke, E. E. Gross, and A. Zucker, Phys. Rev. 163, 1153 (1967).

[14]L. L. Rutledge, Jr. and J. C. Hiebert, Phys. Rev. C 13, 1072 (1976).

[15]M. L. Goldberger and K. M. Watson, *Collision Theory* (Wiley, New York, 1964).

[16]H. Sherif, Nucl. Phys. A131, 532 (1969); W. G. Love,

ibid. A192, 49 (1972), and references therein.

[17]R. P. Liljestrand *et al.*, Phys. Rev. Lett. 42, 363 (1979).

[18]G. S. Adams *et al.*, Phys. Rev. Lett. 43, 421 (1979).

[19]J. J. Simpson *et al.*, Phys. Rev. Lett. 35, 23 (1975), and references therein; P. Braun-Munzinger *et al.*, *ibid.* 21, 1261 (1972).

[20]L. Ray *et al.*, Phys. Rev. Lett. 40, 1547 (1978).

[21]L. Ray *et al.*, Phys. Lett. 83B, 275 (1979).

[22]G. S. Adams *et al.*, Phys. Rev. Lett. 38, 1387 (1977), and references therein.

[23]N. Hintz, private communication.

[24]R. Lindgren, private communication.

[25]R. M. Haybron, M. B. Johnson, and R. J. Metzger, Phys. Rev. C 156, 1136 (1967).

[26]A. Scott, N. P. Mathur, and F. Petrovich, Nucl. Phys. A285, 222 (1977); Y. Terrien, *ibid.* A199, 65 (1973); G. R. Hammerstein, R. H. Howell, and F. Petrovich, *ibid.* A213, 45 (1973); R. Schaeffer, *ibid.* A135, 231 (1969); see also the references in the above.

[27]I. Amhad, Nucl. Phys. A247, 418 (1975).

[28]T. S. Bauer *et al.*, Phys. Rev. C 19, 1438 (1979), and references therein.

[29]Richard Schaffer, *The Two-Body Force in Nuclei*, edited by S. M. Austin and G. M. Crawley (Plenum, New York, 1972), p. 245; F. Petrovich, V. A. Madsen, and J. Atkinson, Phys. Rev. Lett. 22, 895 (1969).

[30]F. Petrovich *et al.*, Phys. Lett. (to be published).

[31]G. D. Alkhazov *et al.*, Nucl. Phys. A274, 443 (1976).

[32]P. L. Hallowell *et al.*, Phys. Rev. C 7, 1396 (1973).

[33]K. Itoh, M. Oyamada, and Y. Torizuka, Phys. Rev. C 2, 2181 (1970).

[34]J. Heisenberg, J. S. McCarthy, and I. Sick, Nucl. Phys. A164, 353 (1971).

[35]G. S. Adams, Ph.D. thesis, Indiana University (1977), or Indiana University Cyclotron Facility Internal Report No. 77-3.

[36]R. F. Frosch *et al.*, Phys. Rev. 174, 1380 (1968).

[37]R. A. Eisenstein *et al.*, Phys. Rev. 188, 1815 (1969).

[38a]J. B. McGrory, B. H. Wildenthal, and E. C. Halbert, Phys. Rev. C 2, 186 (1970).

[38b]This ratio is consistent with the isoscalar transition rate one deduces from (α, α') data [see A. M. Bernstein, in *Advances in Nuclear Physics*, edited by M. Baranger and E. Vogt (Plenum, New York, 1969), Vol. 3, p. 325].

[39]Phan-Xuan-Ho, J. Bellicard, and Ph. Leconte, Nucl. Phys. A210, 189 (1973).

[40]I. Morrison, R. Smith, and K. Amos, Nucl. Phys. A244, 189 (1975).